23rd ABCM International Congress of Mechanical Engineering
December 6-11, 2015, Rio de Janeiro, RJ, Brazil

FLEXURAL WAVE BAND GAPS IN METAMATERIAL ELASTIC BEAM

Edson Jansen Pedrosa de Miranda Júnior
José Maria Campos dos Santos
VibroAcoustics Laboratory, Department of Computational Mechanics, University of Campinas, Mendeleyev Street, 200, Cidade Universitária “Zeferino Vaz”, Barão Geraldo, 13083860, Campinas – SP, Brazil
edson.jansen@ifma.edu.br, zema@fem.unicamp.br

Abstract. *In the last decades, many researches have been done to the field of wave propagation in periodic structures. More recently these researches have been focused in metamaterials. Metamaterials are heterogeneous materials which are made of various materials with periodic distribution. Due to its periodic structure, some frequency ranges may exist where elastic or acoustic waves are forbidden to propagate (band gaps). In this paper, we demonstrated the formation of band gaps and spectral attenuation of flexural waves in metamaterial elastic beam with periodically variation of two materials. This metamaterial features a unique wave filtering characteristics that can find applications to vibration and acoustic control. The study is performed by using five approaches, the transfer-matrix method (MTM), the finite element method (FEM), the spectral element method (SEM) ,the wave finite element method (WFEM) and the wave spectral element method (WSEM), to predict the propagation constants and the complex band structures. Finite periodic structure is considered. Results are discussed and compared to each other.*

Keywords: *metamaterial elastic beams, band gaps, periodic structures, vibration and acoustic control.*

1. INTRODUCTION

Elastic wave propagation in periodic structures has been studied for decades (MEAD, 1975; MEAD, 1996; BRILLOUIN, 1953). It is well known that such structures feature wave filtering properties, thus waves cannot propagate freely through the periodic structures within some frequency ranges, which are called band gaps or stop bands (XIAO *et al.*, 2012). This property is important to many applications such as acoustics and mechanical wave filters, acoustic barriers, vibration isolators, etc.

In recent years, periodic composite materials known as phononic crystals (PCs), consisting of a periodic array of acoustic scatterers embedded in a host medium, have received renewed attention because PCs exhibit complete elastic band gaps within which sound and vibration are all forbidden (LIU *et al.*, 2007).

The PCs are a type of metamaterials. According to Vescovo and Giorgio (2014), metamaterials are materials which are designed to have exotic behavior: the concept has been first conceived for optical and devices. Therefore, very often one talk about mechanical metamaterials, when the exotic behavior is limited to mechanical effects, as *e.g.* very negative Poisson effects. The use of the word *metamaterial* in this paper is intended as a synonym of PCs.

In PCs investigation, two kinds of band gap formation mechanism have been developed. Earlier investigations are focused on band gaps based on the Bragg scattering mechanism or Bragg reflection mechanism (RICHARDS AND PINES, 2003; WEN *et al.* 2005). This type of band gaps are called Bragg type gaps, whose frequency location is governed by the Bragg condition $d=n(\lambda/2)$ $(n=1,2,3,\ldots)$, where d is the lattice constant of the periodic system, and λ is the wavelength of the waves in the host material.

The Bragg condition implies that, to realize a Bragg gap in PCs, the spatial modulation of the elasticity must be of the same order as the relevant wavelength. Thus is difficult to achieve a low frequency Bragg gap in PCs with a small size (XIAO *et al.* 2012).

Recently, in contrast, Liu *et al.* (2000) have proposed a type of locally resonant (LR) PC containing an array of resonant units. Resonance-type band gaps were obtained in a frequency range two orders of magnitude lower than that given by the Bragg limit. More recently, the investigation of LR PCs has been extended to a newly emerging field: acoustic metamaterials (AMs). The negative effective acoustic properties of LR AMs have attracted increasing attention (YAO *et al.*, 2008; HUANG and SUN, 2010; PAI, 2010; ZHU *et al.* 2011).

In this paper, we consider a free-free Euler-Bernoulli beam containing a periodic array of cells. Each cell is composed by two materials, in this case steel and polyethylene. The main purpose of the present paper is to analyze the Bragg gap formation and the dispersion relation of a finite beam using the transfer-matrix method (MTM), the finite element method (FEM), the spectral element method (SEM), the wave finite element method (WFEM) and the wave spectral element method (WSEM).

2. THE MODEL AND THE METHOD

Figure 1 sketches a metamaterial beam with periodic array of cells of two different materials. The lattice constant of the periodic system is d. Each cell is composed by 2/3 of steel and 1/3 of polyethylene.

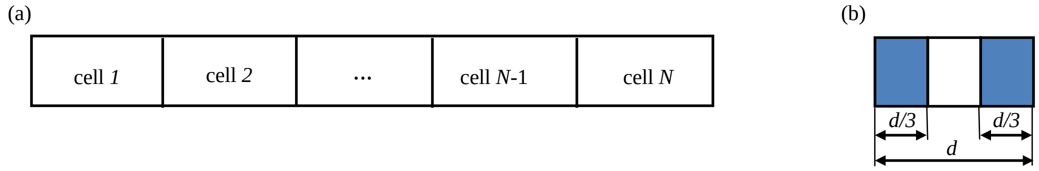

Figure 1. (a) Schematic representation of a metamaterial elastic beam with N unit cells. (b) One unit cell of the system.

2.1 Wave finite element method (WFEM)

Figure 2 presents a waveguide divided into cells/slices/substructures. The length of each substructure, along x direction, is denoted as d. Each left and right boundaries of interface of substructures contain the same number degrees of freedom (DOFs) – n.

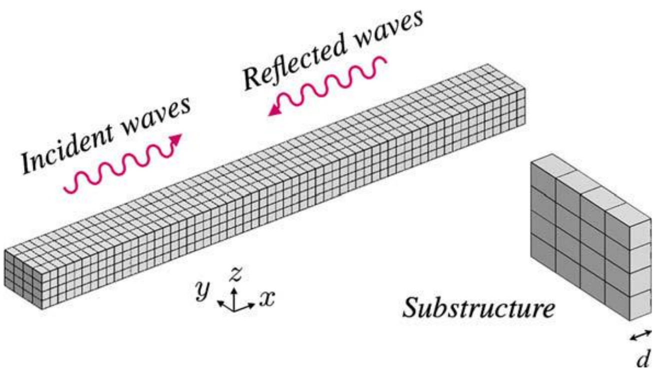

Figure 2. Illustration of incident and reflected waves in a waveguide divided into substructures (MENCIK, 2010).

The dynamic equilibrium of the cell is:

$$\boldsymbol{Dq} = \boldsymbol{F} \tag{1}$$

where $\boldsymbol{D} = (1 + i\eta)\boldsymbol{K} - w^2\boldsymbol{M}$ is the dynamic stiffness matrix, $\boldsymbol{q}$ is the vector of displacements and rotations, $\boldsymbol{F}$ is the vector of forces and moments, $\boldsymbol{M}$ is the mass matrix, $\boldsymbol{K}$ is the stiffness matrix, η is the damping or the loss factor and w is the angular frequency. Following the theory of Zhong and Williams (1995), the dynamic equilibrium equation can be reformulated in terms of state vectors:

$$\boldsymbol{u}_R = \boldsymbol{S}\boldsymbol{u}_L \tag{2}$$

where $\boldsymbol{S}$ is the transfer matrix, a ($2n$ x $2n$) symplectic matrix, the subscripts L and R refer to as the left and right boundaries, while:

$$\boldsymbol{S} = \begin{bmatrix} -(\boldsymbol{D}_{LR}^*)^{-1}\boldsymbol{D}_{LL}^* & -(\boldsymbol{D}_{LR}^*)^{-1} \\ \boldsymbol{D}_{RL}^* - \boldsymbol{D}_{RR}^*(\boldsymbol{D}_{LR}^*)^{-1}\boldsymbol{D}_{LL}^* & -\boldsymbol{D}_{RR}^*(\boldsymbol{D}_{LR}^*)^{-1} \end{bmatrix}, \ \boldsymbol{u}_L^T = \begin{bmatrix} (\boldsymbol{q}_L)^T \\ (-\boldsymbol{F}_L)^T \end{bmatrix}, \ \boldsymbol{u}_R^T = \begin{bmatrix} (\boldsymbol{q}_R)^T \\ (\boldsymbol{F}_R)^T \end{bmatrix} \tag{3}$$

where $\boldsymbol{D}^*$ refers to as the dynamic stiffness matrix of cell condensed onto its left and right boundaries. Using the coupling conditions between two consecutive substructures k and k-1, say:

$$\boldsymbol{u}_L^{(k)} = \boldsymbol{u}_R^{(k-1)} \tag{4}$$

and in Eq. (2) leads to:

$$\boldsymbol{u}_L^{(k)} = \boldsymbol{S}\boldsymbol{u}_L^{(k-1)} \tag{5}$$

From Bloch's theorem (WILCOX, 1978), the solutions of Eq. (5) are denoted as $\{(\mu_j, \boldsymbol{\Phi}_j)\}_j$ and refer to as the wave modes traveling along the global structure. They are numerically computed by means of the following eigenvalue problem:

$$\boldsymbol{S\Phi}_j = \mu_j \boldsymbol{\Phi}_j, \qquad |(\boldsymbol{S} - \mu_j \boldsymbol{I})| = 0 \tag{6}$$

where the eigenvector associated with the eigenvalue μ_j is denoted by:

$$\boldsymbol{\Phi}_j = \begin{bmatrix} \boldsymbol{q}(\mu_j) \\ \boldsymbol{F}(\mu_j) \end{bmatrix} = \begin{bmatrix} (\boldsymbol{\Phi}_q)_j \\ (\boldsymbol{\Phi}_F)_j \end{bmatrix} \tag{7}$$

For a given mode j, the scalar parameter μ_j is related to wavenumber because $\mu_j = exp(-ik_j d)$, while the eigenvector $\boldsymbol{\Phi}_j$ represents the wave shape. The eigenvalue problem in Eq. (6) is ill-conditioned, therefore Zhong and Williams (1995) proposed an homogeneous generalized eigenvalue problem of following form:

$$\boldsymbol{Nw}_j = \mu_j \boldsymbol{Lw}_j, \qquad |\boldsymbol{N} - \mu_j \boldsymbol{L}| = 0 \tag{8}$$

Since the matrix $\boldsymbol{S}$ is symplectic, its eigenvalues come in pair as (μ_j, $1/\mu_j$) for $j=1,\dots,n$. Furthermore, in real structures, some damping is always present. Thus,

- If $|\mu_j|<1$, the wave propagates to the right.
- If $|\mu_j|>1$, the wave propagates to the left.

If there is no damping, thus:

- When $|\mu_j|=1$, the wave propagates to the right if $real(iw\boldsymbol{\Phi}_q^H \boldsymbol{\Phi}_F)<0$.
- When $|\mu_j|=1$, the wave propagates to the left if $real(iw\boldsymbol{\Phi}^{*H}_q \boldsymbol{\Phi}^*_F)>0$.

The Modal Assurance Criterion (MAC) is used for estimating the correlation among wave shapes. Given a wave mode j defined at angular frequency w and for a small Δ_w, wave mode j defined at angular frequency $w+\Delta_w$ is such that:

$$\left| \frac{\boldsymbol{\Phi}_j(w)^H}{\|\boldsymbol{\Phi}_j(w)\|} \frac{\boldsymbol{\Phi}_j(w+\Delta_w)}{\|\boldsymbol{\Phi}_j(w+\Delta_w)\|} \right| = max_k \left\{ \left| \frac{\boldsymbol{\Phi}_j(w)^H}{\|\boldsymbol{\Phi}_j(w)\|} \frac{\boldsymbol{\Phi}_k(w+\Delta_w)}{\|\boldsymbol{\Phi}_k(w+\Delta_w)\|} \right| \right\} \tag{9}$$

According to Duhamel *et al.* (2006) and Mencik (2010), the left state vector is given by the sum of the positive and negative-going waves:

$$\boldsymbol{u}_L^{(k)} = \sum_{j=1}^{n} Q_{Lj} \boldsymbol{\Phi}_j + Q_{Lj}^* \boldsymbol{\Phi}_j^* \tag{10}$$

and the right state vector is given by:

$$\boldsymbol{u}_R^{(k)} = \sum_{j=1}^{n} Q_{Rj} \boldsymbol{\Phi}_j + Q_{Rj}^* \boldsymbol{\Phi}_j^* \tag{11}$$

where * indicates the direction of the negative-going waves. Mencik (2010) mentions this because of symmetry properties (only works when the left and the right sides of the substructure are symmetric to each other):

$$(\boldsymbol{\Phi}_q^*)_j = R(\boldsymbol{\Phi}_q)_j, \quad (\boldsymbol{\Phi}_F^*)_j = -R(\boldsymbol{\Phi}_F)_j \tag{12}$$

where R is a (n x n) symmetry transformation matrix.

2.2 Wave spectral element method (WSEM)

The formulation is the same of WFEM for Euler-Bernoulli beams, but in WSEW the dynamic stiffness matrix is derived from spectral element method (SEM) formulation (DOYLE, 1997; LEE, 2009).

2.3 Transfer-matrix method (MTM)

The transfer-matrix method has been extensively used to solve periodic structures dynamics problems. Instead of relating forces and displacements at the extremities of an element as done in FEM or SEM, the transfer matrix relates the state vector of displacements and forces at a node with forces and displacement at a neighboring node, as represented in Eq. (5). Furthermore, assembling the global matrix is done by propagating the transfer matrices from element 1 to N:

$$\boldsymbol{S}_G = \boldsymbol{S}_{(N+1)N} \ldots \boldsymbol{S}_{32}\boldsymbol{S}_{21} \tag{13}$$

where the matrix $\boldsymbol{S}_G$ relates:

$$\boldsymbol{u}_L^{(N+1)} = \boldsymbol{S}_G \boldsymbol{u}_L^{(1)} \tag{14}$$

Applying the boundary conditions, free-free in this paper, the Eq. (14) could be written in the following form:

$$\begin{bmatrix} -\left(\boldsymbol{D}^*_{LR\,G}\right)^{-1}\boldsymbol{D}^*_{LL\,G} & \left(\boldsymbol{D}^*_{LR\,G}\right)^{-1} \\ -\left(\boldsymbol{D}^*_{RR\,G}\right)^{-1}\boldsymbol{D}^*_{RL\,G} & \boldsymbol{0} \end{bmatrix} \begin{bmatrix} \boldsymbol{q}_L^{(1)} \\ \boldsymbol{q}_L^{(N+1)} \end{bmatrix} = \boldsymbol{F}_L \begin{bmatrix} \boldsymbol{1} \\ \boldsymbol{1} \end{bmatrix} \tag{15}$$

where $\boldsymbol{F}_L$ is the input signal, in this case the vector of forces and moments of the left side of the structure.

Instead of calculating the shape modes and the eigenvalues of Eq. (8) and calculating the state vector from sum of the waves it's possible to obtain the state vector direct from Eq. (14), but the problem is that matrix $\boldsymbol{S}_G$ and matrix of Eq. (15) are ill-conditioned. In addition, it's possible to obtain $\boldsymbol{S}_G$ from the dynamic stiffness matrix of FEM or SEM. In this paper, it was used $\boldsymbol{S}_G$ from the dynamic stiffness matrix of SEM.

3. RESULTS AND DISCUSSION

For the numerical simulations presented in this section, a beam with length L=0.5 m, square section area A=50x10^{-6} m^2, second moment of inertia I=2.0833x10^{-10} m^4, elasticity modulus E_1=20x10^{10} Pa, E_2=0.48x10^9 Pa, density ρ_1=7700 kg/m^3, ρ_2=935 kg/m^3, loss factor η_1=0.0013, η_2=0.01 and Poisson's ratio υ_1=0.27, υ_2=0.35, where subscript 1 refers to steel and subscript 2 refers to polyethylene. The beam was initially divided into 20 cells, and each cell with 2/3 of steel and 1/3 of polyethylene. Considering WFEM and FEM, it's important to mention that each part of the unit cell described in Fig. (1b) was initially divided into two finite elements. All simulation was implemented in Matlab®.

The forced response of the beam was analyzed considering a free-free boundary condition and a signal force as a cosine-shaped pulse only on the left side of the beam. Figure (3a) presents the signal response in displacement and the rotation of the left side of beam. The fact that the MTM has problems of ill-condition could be observed after 480 Hz.

Figure (3b) shows the ill-condition of the matrixes in Eq. (14) and Eq. (15), called of matrix 1 and matrix 2, respectively. It was used the Lapack reciprocal condition estimator to analyze the condition of the matrix. If the estimator is near 1.0, the matrix is well conditioned or 0, assuming the graphic is in dB.

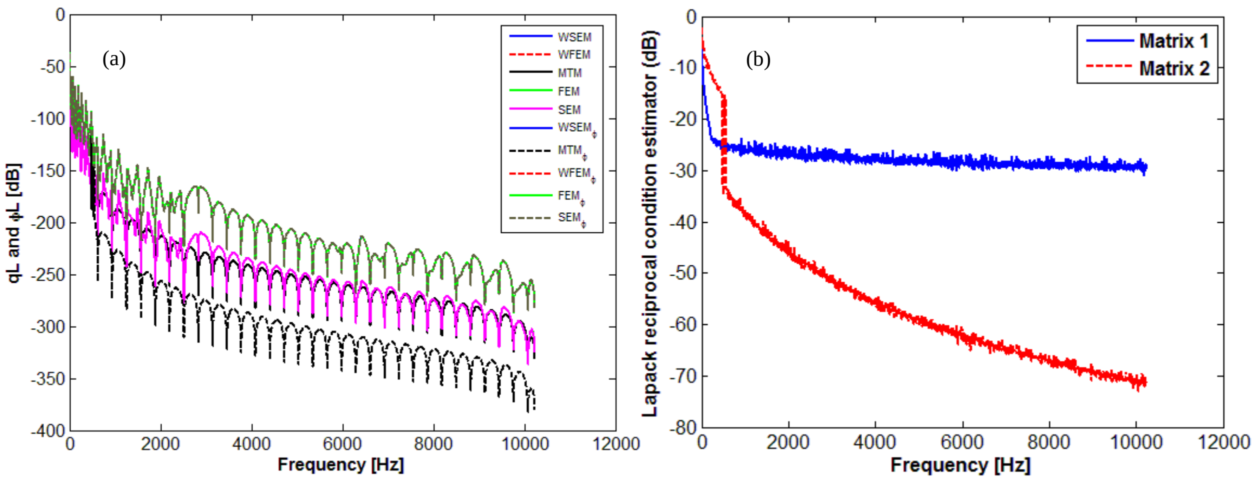

Figure 3. Displacement and rotation frequency response of the left side of the beam (a) and the ill-condition of the matrixes of Eq. (14) and Eq. (15), called of matrix 1 and matrix 2, respectively (b).

The ill-condition increases with frequency. This happens in beam case mainly because of the evanescence waves and considering free-free boundary condition. Thus the others results won't present the MTM.

Figure (4a) shows the signal response in displacement and the rotation of the right side of beam. The magnitude decreasing of the displacement and the rotation happen because of the band gap formation. The range of frequency of band gap formation is better analyzed in transmittance or receptance graphics.

Figure (4b) shows the displacement transmittance and the rotation transmittance of the beam. The band gap formation is observed between 2830 and 5645 Hz approximately.

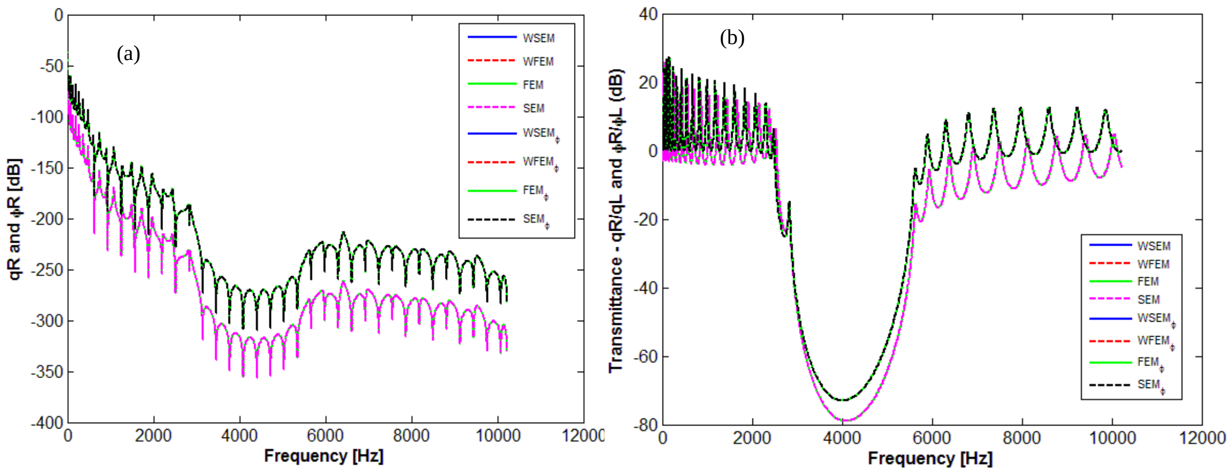

Figure 4. Displacement and rotation frequency response of the right side of the beam (a) and transmittance of the displacement and rotation of the beam (b).

Figure (5) shows the displacement receptance and the rotation receptance of the beam.

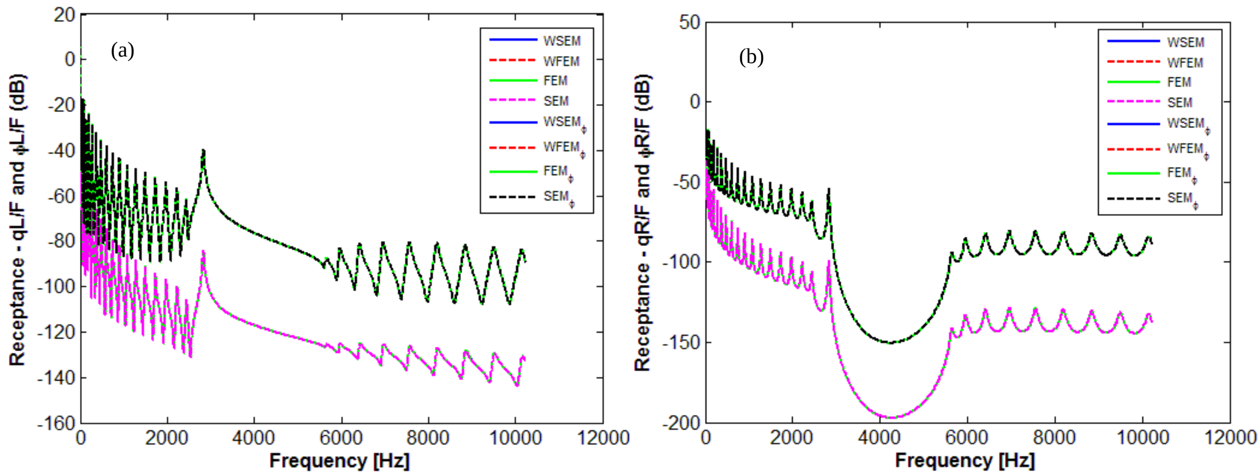

Figure 5. Receptance of the left side (a) and of the right side (b) of the beam.

The dispersion relation or the complex band structure of the metamaterial elastic beam can be observed in Fig. (6). The first Bragg frequency can be calculated using the Bragg condition $d=n(\lambda/2)$ or $kd=n\pi$ $(n=1)$:

$$f_{B1} = \frac{1}{2\pi}\left(\frac{\pi}{d}\right)^2 \sqrt{\frac{EI}{\rho A}} \tag{16}$$

However, in this case, we cannot apply Eq. 16 directly because the unit cell is composed by two different materials and the f_{B1} is not a single point anymore. The Bragg condition *(n=1)* is valid for a range of frequency, in this case is approximately $\Delta f_{B1}=[2750; 5210]$ Hz. The complex band structure of the metamaterial elastic beam observed in Fig. (6) assumes only the positive values of *k*, in other words the positive part of the first Brillouin zone.

Another interesting parameter investigated was the number of unit cells. Figure (7) shows the displacement transmittance of the beam divided into 4, 8 and 20 cells. Considering WFEM and FEM for 4 and 8 cells each part of the unit cell described in Fig. (1b) was divided in twelve finite elements.

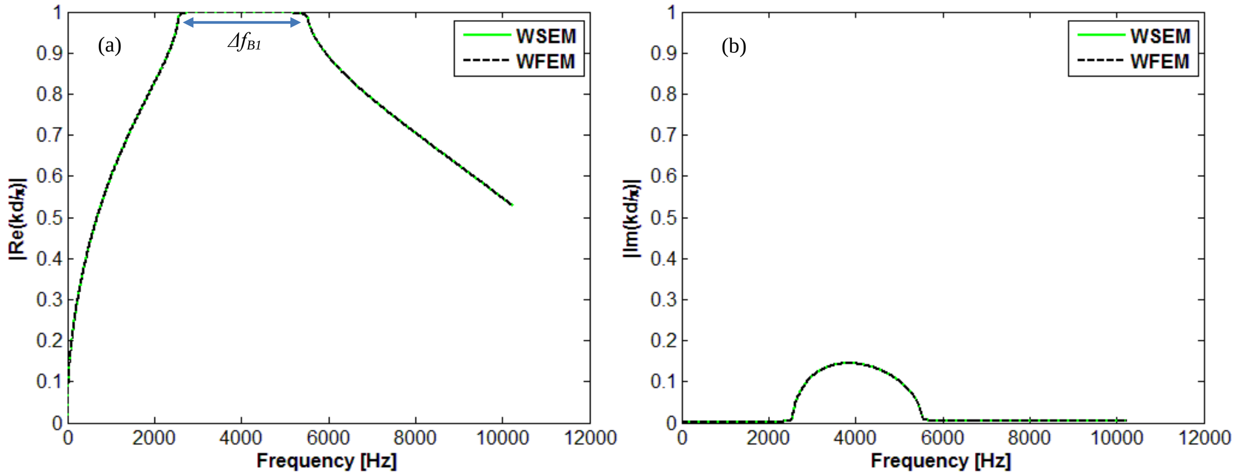

Figure 6. Complex band structure of the metamaterial elastic beam.

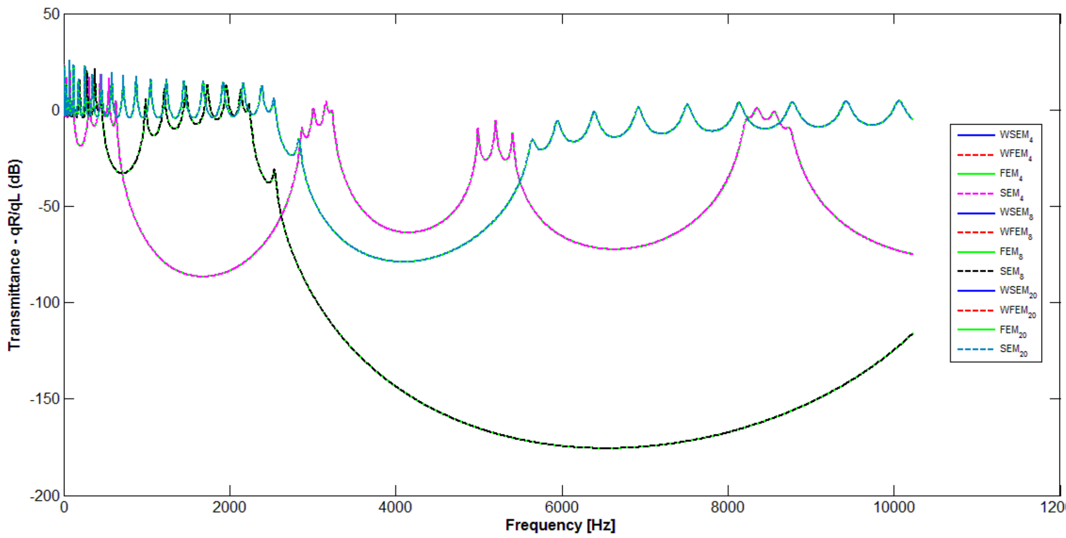

Figure 7. Transmittance of the beam displacement with 4 (pink), 8 (black) and 20 (blue) unit cells.

It is possible to achieve band gaps formation in low frequencies considering a small number of unit cells. Furthermore, the band gaps formation assuming a great number of unit cells it is possible to be achieved in higher frequencies. Figure (8) and Fig. (9) show the complex band structure of the metamaterial elastic beam with 8 and 4 unit cells, respectively.

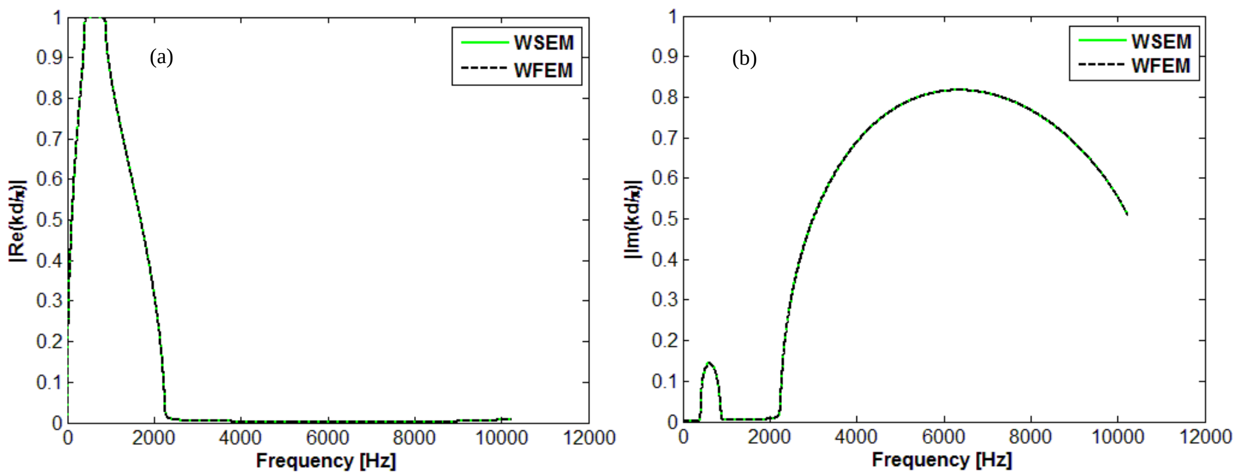

Figure 8. Complex band structure of the metamaterial elastic beam with 8 unit cells.

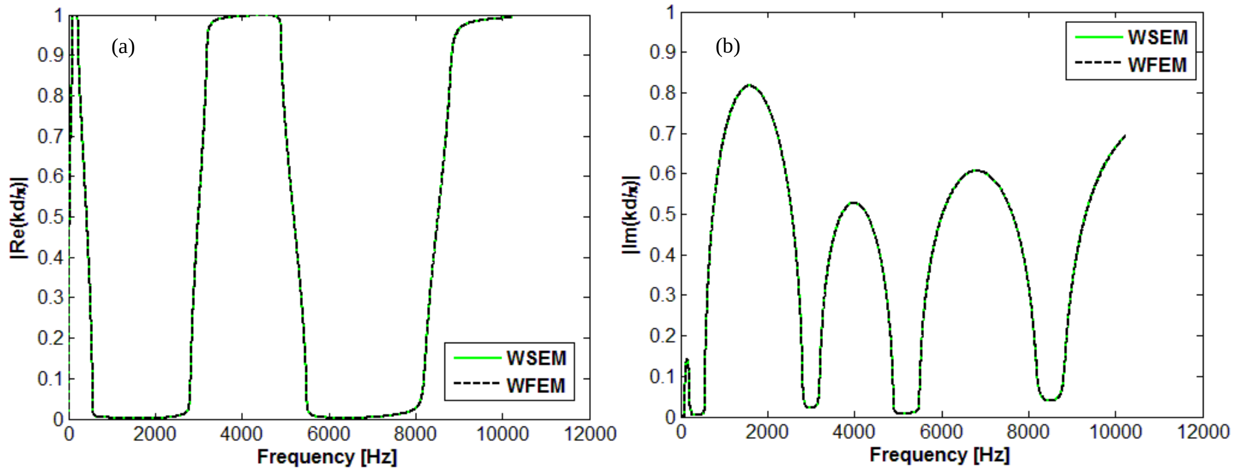

Figure 9. Complex band structure of the metamaterial elastic beam with 4 unit cells.

Figure (10) shows the attenuation constant surface of the metamaterial elastic beam with 4 (a), 8 (b), 20 (c) and 30 (d) unit cells varying from 5% to 95% of polyethylene, where d_{pol} is the length of the polyethylene, d is the length of the cell and the attenuation constant is defined as $\mu=-ikd$. It wasn't used a nondimensional frequency $\Omega=(d/\pi)(\rho/E)^{1/2}w$ because the cell has two materials. The attenuation constant surface was calculated using WSEM.

It must be observed that the attenuation constant, μ, is different from the eigenvalues μ_j defined in the beginning of the paper. In fact $\mu_j=exp(\mu)$, thus the imaginary part of the Bloch wave vector (or the cell wavenumber), $Im(k)$, which quantifies the wave attenuation per unit of length is related to the attenuation constant by the relation: $Re(\mu)= Im(k)L$.

The comportment of the attenuation is complex and varies with the number of unit cells. The density of the attenuation regions increases with the decreasing number unit cells.

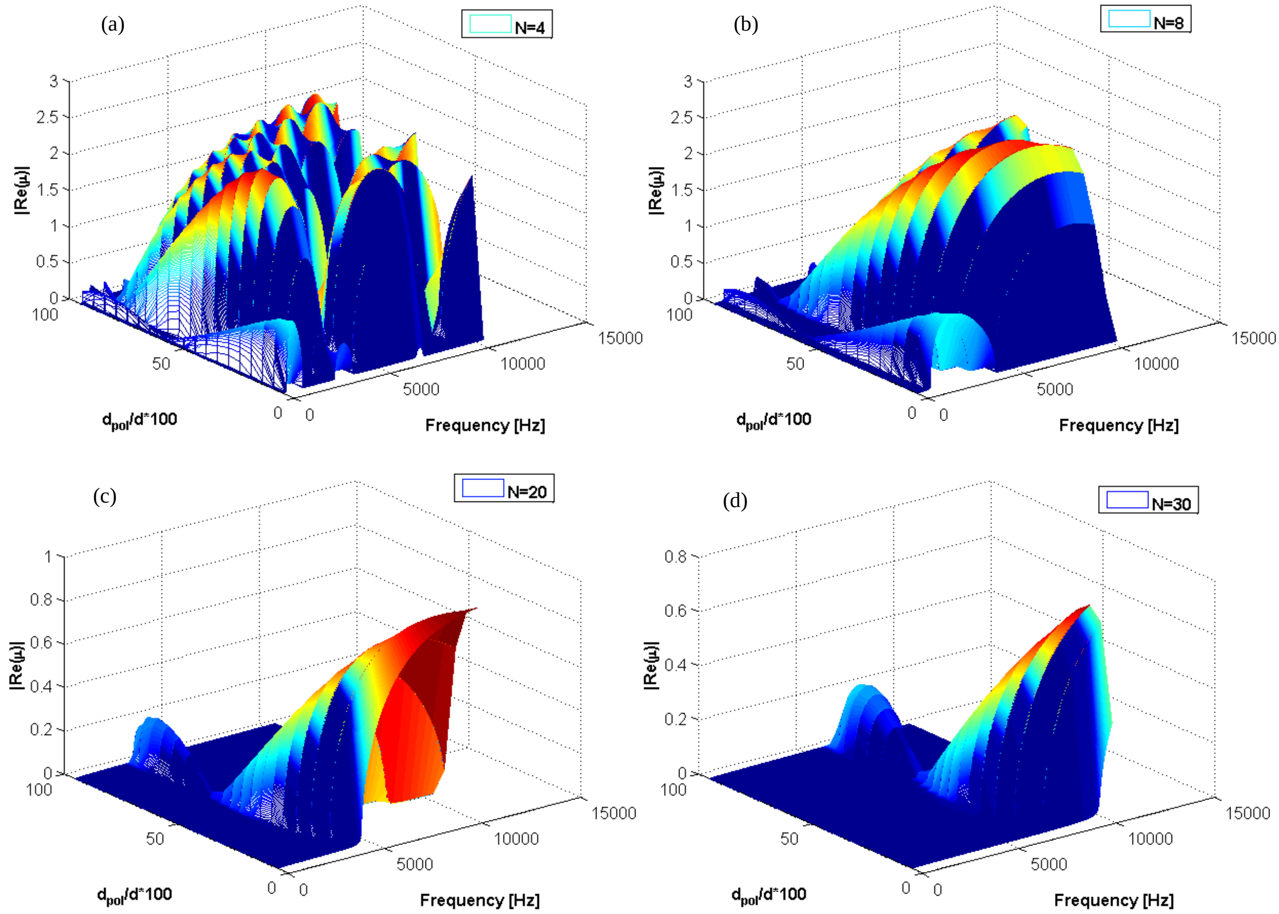

Figure 10. Attenuation constant surface of the metamaterial elastic beam with 4 (a), 8 (b), 20 (c) and 30 (d) unit cells using WSEM.

The attenuation is higher for values smaller than 50% of polyethylene. Considering 4 or 8 unit cells it is possible to achieve great attenuations in low frequencies. Taking into account 20 and 30 unit cells the greater attenuations occurs to a low quantity of polyethylene in higher frequencies. However, considering 4 and 8 unit cells the greater attenuations occurs close to 50% of polyethylene. Furthermore, the greater attenuations assuming a high number of unit cells it is possible to be achieved in higher frequencies.

4. CONCLUSIONS

In this study, the band gap formation was observed in a range of frequency of 2830 and 5645 Hz. The results of MTM were not satisfactory because of the ill-condition of the matrixes in Eq. 14 and Eq. 15. All the others methods – FEM, SEM, WFEM and WSEM – presented the same results. It was possible to achieve Bragg gaps formation in low frequencies considering a small number of unit cells. Considering 4 or 8 unit cells, WFEM and FEM converge with WSEM and SEM assuming 11 internal degrees of freedom in each part of the unit cell.

The comportment of the attenuation is complex and varied with the number of unit cells. The best attenuation was found to 4 unit cells with approximately 50% of polyethylene. The findings presented indicate the potential of using periodic structures with discontinuities to achieve band gap formation. However, should be mention that is difficult to achieve a low frequency Bragg gap in metamaterials with a small size.

5. REFERENCES

Brillouin, L., 1953. *Wave Propagation in Periodic Structures*. Dover, New York, 2nd edition.

Doyle, J.F., 1997. *Wave Propagation in Structures: Spectral Analysis Using Fast Discrete Fourier Transforms.* Springer-Verlag, New York, 2nd edition.

Duhamel, D., Mace, B.R., and Brennan, M.J., 2006. "Finite element analysis of the vibrations of waveguides and periodic structures". *Journal of Sound and Vibration,* Vol. 294, p. 205-220.

Lee, U., 2009. *Spectral Element Method in Structural Dynamics.* John Wiley & Sons, Singapore.

Liu, Z., Zhang, X., Mao, Y., Zhu, Y.Y., Yang, Z. and Chan, C.T., 2000. "Locally resonant sonic materials". *Science.* Vol. 289, p. 1734.

Liu, Y., Yu, D., Li, L., Zhao, H., Wen, J. and Wen, X., 2007. "Design guidelines for flexural wave attenuation of slender beams with local resonators". *Physics Letters A,* Vol. 362, p. 344-347.

Huang, G.L. and Sun, C.T., 2010. "Band gaps in a multiresonator acoustic metamaterial". *Journal of Vibration and Acoustics*, Vol. 132, p. 031003.

Mead, D.J., 1975. "Wave propagation and natural modes in periodic systems: I mono-coupled systems". *Journal of Sound and Vibration,* Vol. 40, p. 1-18.

Mead, D.J., 1996. "Wave propagation in continuous periodic structures: research contributions from Southampton". *Journal of Sound and Vibration,* Vol. 190, p. 495-524.

Mencik, J.M., 2010. "On the low- and mid-frequency forced response of elastic structures using wave finite elements with one dimensional propagation". *Computers and Structures,* Vol. 88, p. 674-689.

Pai, P.F., 2010. "Metamaterial-based broadband elastic wave absorber". *Journal of Intelligent Material Systems and Structures,* Vol. 21, p. 517-528.

Richards, D. and Pines, D.J., 2003. "Passive reduction of gear mesh vibration using periodic drive shaft". *Journal of Sound and Vibration,* Vol. 264, p. 317-342.

Vescovo, D.D. and Giorgio, I., 2014. "Dynamic problems for metamaterials: review of existing models and ideas for further research". *International Journal of Engineering Science,* Vol. 80, p. 153-172.

Wen, J., Wang, G., Yu, D., Zhao, H. and Liu, Y., 2005. "Theorical and experimental investigation of flexural wave propagation in straight beams with periodic structures: application to a vibration isolation structure". *Journal of Applied Physics.* Vol. 97, p. 114907.

Wilcox, C., 1978. "Theory of Bloch waves". *Journal d'Analyse Mathématique,* Vol. 33, p. 146 – 167.

Xiao, Y., Wen, J. and Wen, X., 2012. "Broadband locally resonant beams containing multiple periodic arrays of attached resonators". *Physics Letters A,* Vol. 376, p. 1384-1390.

Yao, S.S., Zhou, X.M. and Hu, G.K., 2008. "Experimental study on negative effective mass ia a 1D mass-spring system". *New Journal of Physics,* Vol. 10, p. 043020.

Zhu, R., Huang, H.H. and Sun, C.T., 2011. "Experimental and numerical study of guided wave propagation in a thin metamaterial plate". *Physical Letters A,* Vol. 375, p. 2863-2867.

Zhong, W.X. and Williams, F.W., 1995. "On the direct solution of wave propagation for repetitive structures". *Journal of Sound and Vibration,* Vol. 181, p. 485-501.

6. RESPONSIBILITY NOTICE

The authors are the only responsible for the printed material included in this paper.